

# Sparticle masses from transverse mass kinks at the LHC: the case of Yukawa-unified SUSY GUTs

---

Kiwoon Choi<sup>a</sup>, Diego Guadagnoli<sup>b</sup>, Sang Hui Im<sup>a</sup> and Chan Beom Park<sup>a</sup>

<sup>a</sup> *Department of Physics, Korea Advanced Institute for Science and Technology, Daejeon 305-701, Korea*

<sup>b</sup> *Excellence Cluster Universe, Technische Universität München, Boltzmannstraße 2, D-85748 Garching, Germany*

*Email: [kchoi@muon.kaist.ac.kr](mailto:kchoi@muon.kaist.ac.kr), [diego.guadagnoli@ph.tum.de](mailto:diego.guadagnoli@ph.tum.de), [shim@muon.kaist.ac.kr](mailto:shim@muon.kaist.ac.kr), [cbpark@muon.kaist.ac.kr](mailto:cbpark@muon.kaist.ac.kr)*

*(Dated: October 29, 2018)*

ABSTRACT: We explore, in a concrete example, to which extent new particle mass determinations are practicable with LHC data. Our chosen example is that of Yukawa-unified SUSY GUTs, whose viability has been recently studied for two general patterns of soft SUSY-breaking terms. We note that both patterns of SUSY spectra do not admit long decay chains, which would make it possible to determine the masses of the SUSY particles involved using endpoints or mass relations. We thus take the so-called  $m_{T2}$ -kink method as our key strategy, since it does not rely on the presence of long decay chains. We then discuss a procedure allowing to determine the masses of the gluino, of the lightest chargino as well as of the first two neutralinos and, for the scenario where a stop is lighter than the gluino, the mass of the light stop too. Our worked example of Yukawa-unified SUSY GUTs may offer a useful playground for dealing with other theories which predict similar patterns of SUSY spectra.

---

## Contents

<b>1. Introduction</b>	<b>1</b>
<b>2. Methods for SUSY mass determinations at the LHC</b>	<b>4</b>
2.1 Methods other than $m_{T2}$	4
2.2 The $m_{T2}$ -kink method	5
2.3 Generalizations	7
<b>3. Strategy</b>	<b>9</b>
3.1 Strategy: LS scenario	9
3.2 Strategy: HS scenario	12
<b>4. Analysis and results</b>	<b>13</b>
4.1 Analysis: LS scenario	13
4.2 Analysis: HS scenario	18
<b>5. Conclusions and Outlook</b>	<b>21</b>

---

## 1. Introduction

Existing data on established collider quantities – in particular electroweak precision tests, quark masses and flavour-changing neutral current processes – provide crucial constraints on many sets of Standard Model (SM) extensions, whose new interactions do in general imply tree- or loop-level deviations in some or all of these observables. These tests allow to learn whether a given class of theories is viable at all, and, if so, to learn about the features of the viable parameter space. However these tests, at present, are mostly null tests, where the chosen class of theories is required to produce a small signal as compared with the SM. It is clear that, in order to single out the considered class of theories, one has to find observables for which an unequivocally different behavior with respect to the SM is predicted. With the imminent flow of direct data from the Large Hadron Collider (LHC), such observables may be found in inclusive searches or, better, in the direct determination of at least the lightest part of the new particles' spectrum. The second possibility is clearly more ambitious, but also much more powerful than the first one to tell apart a given theory against other possibilities. Aim of the present paper is to explore, in a concrete example, to which extent new particles' mass determinations are practicable with LHC data.

The example we focus on is that of supersymmetric (SUSY) grand unified theories (GUTs) with Yukawa unification (YU), whose viability and expected signatures have been

extensively studied with different approaches for various general patterns of soft SUSY-breaking terms [1, 2, 3, 4, 5, 6, 7, 8, 9, 10, 11, 12, 13, 14, 15, 16, 17, 18, 19].<sup>1</sup> We will focus here on the two scenarios considered in refs. [10] and [16], that we briefly summarize in the rest of this section. In ref. [10] the case where soft-breaking terms for sfermions and gauginos are universal at the GUT scale was considered. It was found

- (a) that this class of theories is phenomenologically viable only by advocating partial decoupling of the sfermion sector, the lightest mass exceeding 1 TeV;
- (b) that phenomenological viability can be recovered without decoupling by relaxing  $t - b - \tau$  unification to  $b - \tau$  unification, equivalent to a parametric departure of  $\tan \beta$  from the value implied by exact YU. This solution is non-trivial since the constraints from  $m_b$  and respectively FCNCs prefer high,  $O(50)$ , and respectively low values of  $\tan \beta$ . Indeed, a compromise solution has been found to exist only for the narrow range  $46 \lesssim \tan \beta \lesssim 48$ , implying that the breaking of  $t - b$  YU must be *moderate*, in the range 10 – 20%;
- (c) that the requirement of  $b - \tau$  unification and the FCNC constraints are enough to make the predictions for the lightest part of the SUSY spectrum robust ones in the interesting region of point (b). These include a lightest stop mass  $\gtrsim 800$  GeV, a gluino mass of about 400 GeV and lightest Higgs, neutralino and chargino close to the lower bounds. Specifically, the lightest neutralino is in the ballpark of 60 GeV, and the lightest chargino about twice as heavy. The rest of the SUSY spectrum lies instead in the multi-TeV regime: in particular first and second generation sfermion masses, that almost do not RGE-evolve from the GUT scale to the Fermi scale, remain of the order of the GUT-scale bilinear mass  $m_{16} \gtrsim 7$  TeV. For an illustrative example of this spectrum, see the leftmost column of table 1.

Ref. [16], instead, explored the complementary case where YU is kept exact, while the requirement of universal soft terms at the GUT scale (not very justified from a theoretical standpoint) is relaxed. Ref. [16] focused on the scenario in which the breaking of universality inherits from the Yukawa couplings, i.e. is of minimally flavor violating type [32, 33]. This general setup allows in particular for a splitting between the up-type and the down-type soft trilinear couplings. Comparison with data revealed for this trilinear splitting scenario the following features [16]:

- (i) agreement with data clearly selects the parametric region with a large  $\mu$ -term and a sizable splitting between the  $A$ -terms. At the price of a slight increase in the fine tuning required to achieve EWSB with precisely the correct value of  $M_Z$ , this scenario allows a substantial improvement on other observables that, on a model-dependent basis, do often require some amount of fine tuning as well;
- (ii) in particular, and quite remarkably, phenomenological viability does not invoke a partial decoupling of the sparticle spectrum, as is the case in the scenario of ref.

---

<sup>1</sup>For earlier literature on the topic of YU within SUSY GUTs, the reader is referred to [20, 21, 22, 23, 24, 25, 26, 27, 28, 29, 30, 31].

Spectrum predictions			
HS scenario, ref. [10]		LS scenario, ref. [16]	
$M_{h^0}$	121	$M_{h^0}$	126
$M_{H^0}$	585	$M_{H^0}$	1109
$M_A$	586	$M_A$	1114
$M_{H^+}$	599	$M_{H^+}$	1115
$m_{\tilde{t}_1}$	783	$M_{\tilde{t}_1}$	192
$m_{\tilde{t}_2}$	1728	$m_{\tilde{t}_2}$	2656
$m_{\tilde{b}_1}$	1695	$m_{\tilde{b}_1}$	2634
$m_{\tilde{b}_2}$	2378	$m_{\tilde{b}_2}$	3759
$m_{\tilde{\tau}_1}$	3297	$m_{\tilde{\tau}_1}$	3489
$m_{\tilde{\chi}_1^0}$	59	$m_{\tilde{\chi}_1^0}$	53
$m_{\tilde{\chi}_2^0}$	118	$m_{\tilde{\chi}_2^0}$	104
$m_{\tilde{\chi}_1^+}$	117	$m_{\tilde{\chi}_1^+}$	104
$M_{\tilde{g}}$	470	$M_{\tilde{g}}$	399

**Table 1:** Spectrum predictions for representative fits of the viable scenarios studied in refs. [10] and [16]. All masses are in units of GeV. Uppercase and lowercase masses stand for pole and respectively  $\overline{\text{DR}}$  masses.

[10], but instead it *requires* various SUSY particles, notably the lightest stop and the gluino, to be very close to their current experimental limits. Specifically, the lightest stop is lighter than the gluino, in the range [100, 200] GeV. This testable difference reflects the substantial difference in the mechanism that makes the two classes of models phenomenologically viable. Ultimately, it maps onto the difference in the assumed form for the GUT-scale soft terms;

(iii) concerning the rest of the spectrum, the predictions for the gluino, the lightest chargino and neutralino masses, as well as those for the heavy part of the SUSY spectrum, are very similar to the corresponding ones in the scenario of [10] (see ref. [16] for further details). Again, because of the cross-fire between the many constraints used, all these spectrum predictions, including those of point (ii), are robust ones.

As already mentioned, this paper is devoted to exploring the possibility of directly measuring the masses of the lightest SUSY particles in the scenarios of refs. [10, 16]. In particular, it will discuss a strategy – applicable already to data collected at the LHC – that permits the determination of the masses of the gluino, the lightest chargino and neutralino and, for the scenario of ref. [16], the lightest stop also. This task clearly requires to focus on *short* decay chains, and makes extensive use of so-called “transverse mass” variables.

Our strategy will be described in section 3, after an introduction to the methods for new particles’ mass determination at hadron colliders, to be presented in the next section.

## 2. Methods for SUSY mass determinations at the LHC

In this section we briefly recall the methods devised so far for new-particles' mass determinations at the LHC, and discuss their relation with our problem of interest. A comprehensive and very recent review can be found in ref. [34].

### 2.1 Methods other than $m_{T2}$

The most straightforward mass-determination method is, in general, to find a peak in the invariant mass distribution of the decay products of the new particle of interest. This is however inapplicable if the final state includes a component that escapes detection, which is our case, because of the missing 'lightest SUSY particle' (LSP).

For decay chains that include LSPs, in order to reconstruct SUSY masses one can exploit kinematic relations involving these masses and the (measured) momenta of the visible particles. Among the strategies devised to this end, a first possibility is given by the so-called *endpoint method* [35, 36, 37, 38, 39, 40, 41, 42, 43]. It is based on the observation that, in a given decay chain, the endpoint values of the invariant mass distributions constructed for visible decay products depend on the masses of the invisible particles as well. A prototype example is provided by the squark decay chain [44]

$$\tilde{q} \rightarrow \tilde{\chi}_2^0 q \rightarrow \tilde{\ell}^\pm \ell^\mp q \rightarrow \tilde{\chi}_1^0 \ell^+ \ell^- q, \quad (2.1)$$

which would be available for  $m_{\tilde{q}} > m_{\tilde{\chi}_2^0} > m_{\tilde{\ell}} > m_{\tilde{\chi}_1^0}$ . Assuming that the four-momenta of the leptons and of the  $q$ -initiated jet can all be determined with reasonable accuracy, the above decay process provides four invariant-mass distributions, i.e. those of  $m_{\ell\ell}$ ,  $m_{q\ell(\text{high})} = \max(m_{q\ell^+}, m_{q\ell^-})$ ,  $m_{q\ell(\text{low})} = \min(m_{q\ell^+}, m_{q\ell^-})$ , and  $m_{q\ell\ell}$ . Then their endpoints can be inverted to give all the four sparticle masses involved in the decay. However this decay mode is kinematically closed for our scenarios of interest, since all the sleptons are (much) heavier than any of the other sparticles involved in eq. (2.1).

Besides, it can be shown that, in order for all the sparticle masses to be, even in principle, *separately* reconstructible, the endpoint method requires necessarily a long decay chain with at least 3 decay steps [45]. If this condition is not fulfilled, the number of measurable invariant masses is smaller than the number of unknown particle masses, and one can at best determine some combinations of mass differences, rather than determining the absolute mass values. A simple example would be a single-step 3-body decay

$$\tilde{\chi}_2^0 \rightarrow \tilde{\chi}_1^0 \ell^+ \ell^-. \quad (2.2)$$

In this case, the dilepton invariant mass has an endpoint equal to  $m_{\tilde{\chi}_2^0} - m_{\tilde{\chi}_1^0}$ . In order to determine  $m_{\tilde{\chi}_2^0}$  and  $m_{\tilde{\chi}_1^0}$  separately, one would need additional kinematic variables as discussed in [44].

A second method is that of *mass relations*<sup>2</sup> [46, 47, 48, 49, 50]. The idea here is that the four-momenta of missing particles in the decay products can be reconstructed by exploiting various constraints including the on-shell constraints on the decay chain.

---

<sup>2</sup>This method is often called the polynomial method.

Provided the number of branches in the decay chain is sufficiently high, the number of constraints can be made to exceed the number of unknowns, and one can solve (or actually fit) for all the unknowns (for a detailed discussion see [45]). For example, in an  $n$ -step cascade decay initiated by a SUSY particle  $Y$ , with each vertex branching into a SUSY particle  $I_i$  and a SM visible particle with (reconstructible) momentum  $p_i$ ,

$$Y \rightarrow I_1 + V(p_1) \rightarrow I_2 + V(p_2) + V(p_1) \rightarrow \dots \rightarrow I_n(k) + V(p_n) + \dots + V(p_1), \quad (2.3)$$

one has  $n + 1$  independent mass-shell constraints, namely

$$k^2 = m_\chi^2, (k + p_n)^2 = m_{I_{n-1}}^2, \dots, (k + p_1 + \dots + p_n)^2 = m_Y^2, \quad (2.4)$$

where  $k$  is the four-momentum of the missing particle  $I_n$ . For  $N$  such events, the number of constraints will be  $N(n + 1)$ , while the number of unknowns will instead be  $4N + (n + 1)$ , i.e. the four-momentum of the missing particle in each event and the  $n + 1$  masses of the SUSY particles which are common to all events. In order for the number of constraints to exceed the number of unknowns, one needs  $n \geq 4$  and also  $N \geq (n + 1)/(n - 3)$ .

A case where the mass-relation method would be more appropriate is that of symmetric  $n$ -step decays of pair-produced SUSY particles,  $Y + \bar{Y}$ , for which one can use the missing transverse momentum constraint also [48, 50]. In this case, again for  $N$  events, the unknowns include as before  $n + 1$  SUSY particle masses which are common to all events, and the four-momenta of the two missing particles in each event, so the total number of unknowns is given by  $(n + 1) + 8N$ . As for the available constraints, for each event one has  $2(n + 1)$  constraints from the mass-shell conditions and two constraints from the missing transverse momentum, so  $2N(n + 1) + 2N$  constraints in total. We then find the number of constraints is equal to or bigger than the number of unknowns if  $n \geq 3$  and  $N \geq (n + 1)/2(n - 2)$ . These observations lead to the conclusion that one needs at least a 3-step or a 4-step cascade decay in order for the mass-relation method to be applicable.

On the other hand, for the scenarios of refs. [10, 16] the predicted SUSY spectra imply that, at the energies available at the LHC, there cannot be any long decay chain ( $n \geq 3$ ) on which the above discussed endpoint or mass-relation methods might realistically be applied. Specifically, the only 3-step cascade decay with sizable number of events is the gluino decay in the scenario of [16],  $\tilde{g} \rightarrow t\tilde{t}_1^* \rightarrow bW\tilde{b}\tilde{\chi}_1^- \rightarrow bqq\bar{b}qq\tilde{\chi}_0$ , which however suffers from very large jet combinatorics. As a result, the mass-relation method simply cannot be used in our case, and the endpoint method can determine at best mass differences.

## 2.2 The $m_{T2}$ -kink method

A third method exists, however, that is able to determine SUSY masses even in the absence of long decay chains. This method, called the  $m_{T2}$ -kink method [51, 52, 53, 54, 55, 56, 57],<sup>3</sup> exploits the fact that the endpoint value of the transverse mass variable  $m_{T2}$ , regarded as a function of the trial mass  $m_\chi$  of the missing particle in the decay products, exhibits a kink at  $m_\chi = m_\chi^{\text{true}}$  [51]. As the endpoint value of  $m_{T2}$  at  $m_\chi = m_\chi^{\text{true}}$  corresponds to the

---

<sup>3</sup>For another method, also applicable to short decay chains, see [58].

mother particle mass, the  $m_{T2}$ -kink method determines both the mother particle mass and the missing particle mass simultaneously. As we will see, applying the  $m_{T2}$ -kink method to pair-produced gluinos in the scenario of [16], while regarding charginos as missing particles, one can determine both the gluino mass and the chargino mass. Likewise, for the scenario of [10], one can consider the  $m_{T2}$ -kink of gluino pairs while regarding the second lightest neutralinos as missing particles. With those masses determined by the  $m_{T2}$ -kink, the rest of the light part of the SUSY spectrum can be determined by applying the endpoint method.

The collider observable  $m_{T2}$  is a generalization of the transverse mass  $m_T$  which has been introduced for decay processes producing invisible particles [59, 60]. Specifically, considering the decay  $Y \rightarrow V(p) + \chi(k)$ , where  $\chi(k)$  is an invisible particle with four-momentum  $k$ , and  $V(p)$  stands for an arbitrary number of visible particles with total four-momentum  $p$ , the transverse mass  $m_T$  is defined as

$$m_T^2 = m_V^2 + m_\chi^2 + 2 \left( \sqrt{m_V^2 + |\vec{p}_T|^2} \sqrt{m_\chi^2 + |\vec{k}_T|^2} - \vec{p}_T \cdot \vec{k}_T \right), \quad (2.5)$$

where  $m_V$  and  $m_\chi$  are the invariant masses of  $V$  and  $\chi$ , respectively. As the four-momentum of  $\chi$  cannot be directly measured, let  $k$  and  $m_\chi^2 \equiv k^2$  denote a trial four-momentum and respectively a trial mass squared for  $\chi$ , which are introduced for the sake of discussion. A key feature of  $m_T$  is that it is bounded by the invariant mass, i.e. the true mother particle mass  $m_Y^{\text{true}}$ , when  $m_\chi$  and  $\vec{k}_T$  take the true values:

$$\begin{aligned} m_T^2(m_\chi = m_\chi^{\text{true}}, \vec{k}_T = \vec{k}_T^{\text{true}}) &\leq (m_Y^{\text{true}})^2 \\ &= m_V^2 + (m_\chi^{\text{true}})^2 + 2 \left( \sqrt{m_V^2 + |\vec{p}_T|^2} \sqrt{(m_\chi^{\text{true}})^2 + |\vec{k}_T^{\text{true}}|^2} \cosh(\eta_V - \eta_\chi^{\text{true}}) - \vec{p}_T \cdot \vec{k}_T^{\text{true}} \right) \end{aligned}$$

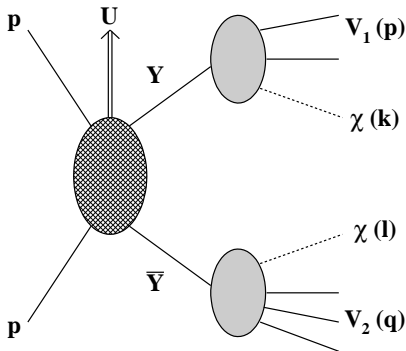


**Figure 1:** Sketch of event topology relevant for the applicability of the  $m_{T2}$ -kink method.

where  $\eta = \frac{1}{2} \ln \left( \frac{E+p_z}{E-p_z} \right)$  is the pseudo-rapidity. While the true momentum of  $\chi$  cannot be directly measured, its transverse component  $\vec{k}_T^{\text{true}}$  can be inferred from the missing transverse momentum if  $\chi$  is the only missing particle in the whole event:  $\vec{k}_T^{\text{true}} = \vec{\cancel{p}}_T$ . Then, once  $m_\chi^{\text{true}}$  is known by some other information, one can determine  $m_Y^{\text{true}}$  from the endpoint value of  $m_T(m_\chi = m_\chi^{\text{true}}, \vec{k}_T = \vec{k}_T^{\text{true}} = \vec{\cancel{p}}_T)$ .

As typical SUSY events involve a pair of SUSY particles decaying into two invisible LSPs, the transverse mass should be accordingly generalized. At the LHC, generic SUSY events take the form (see fig. 1)

$$\begin{aligned} p + p &\rightarrow U + Y + \bar{Y} \\ &\rightarrow U + V_1(p) + \chi(k) + V_2(q) + \chi(l), \end{aligned} \quad (2.6)$$

where  $U$ , often called the upstream momentum, denotes the total four-momentum of visible particles not coming from the decays of the SUSY particle pair  $Y + \bar{Y}$ ,  $\chi$  is the invisible

LSP, and again each  $V_i$  ( $i = 1, 2$ ) denotes an arbitrary number of visible particles produced by the decay of  $Y$  or of  $\bar{Y}$ . (The upstream momentum might come from initial or final state radiation or from the decay of a heavier SUSY particle.) Unlike the case of single missing particle, the transverse momentum of each LSP cannot be determined in this case, although their sum can be read off from the missing transverse momentum. One can then introduce trial LSP transverse momenta,  $\vec{k}_T$  and  $\vec{l}_T$ , under the constraint  $\vec{k}_T + \vec{l}_T = \vec{\cancel{p}}_T$ , and consider the transverse mass of each decay mode. Then the  $m_{T2}$  variable for a trial LSP mass  $m_\chi$  can be constructed as [59, 60]

$$m_{T2}(\text{event}; m_\chi) \equiv \min_{\vec{k}_T + \vec{l}_T = \vec{\cancel{p}}_T} \left[ \max \left( m_T(Y \rightarrow V_1 + \chi), m_T(\bar{Y} \rightarrow V_2 + \chi) \right) \right], \quad (2.7)$$

where each event is specified by the set of *measured* kinematic variables  $\{m_{V_1}, \vec{p}_T, m_{V_2}, \vec{q}_T, \vec{\cancel{p}}_T\}$ , with  $\vec{\cancel{p}}_T$  the total missing transverse momentum. Note that, due to the relation  $\vec{\cancel{p}}_T = -\vec{p}_T - \vec{q}_T - \vec{U}_T$ , use of  $\vec{\cancel{p}}_T$  as an event variable is equivalent to using the upstream transverse momentum  $\vec{U}_T$ . One can now observe two main properties of the  $m_{T2}$  variable: (a) once the rest of the input is fixed (i.e. given the event),  $m_{T2}$  is a monotonic (increasing) function of the trial LSP mass; (b) when the trial LSP mass is equal to the true LSP mass,  $m_{T2}$  is bounded from above by the true mother-particle mass  $m_Y^{\text{true}}$ .

It follows that, studying  $m_{T2}$  as a function of  $m_\chi$  in the neighborhood of  $m_\chi = m_\chi^{\text{true}}$ , and recalling that  $m_{T2}(m_\chi = m_\chi^{\text{true}}) \leq m_Y^{\text{true}}$ , one will observe a kink structure at the point  $\{m_{T2}, m_\chi\} = \{m_Y^{\text{true}}, m_\chi^{\text{true}}\}$ , because the  $m_{T2}$  curves generally feature different slopes at  $m_\chi = m_\chi^{\text{true}}$ . See fig. 2 for an illustration. In fact, a relevant issue for the  $m_{T2}$ -kink method is how sharp the kink is, which is equivalent to how much the slopes of  $m_{T2}$  curves (at  $m_\chi = m_\chi^{\text{true}}$ ) vary over the available event set. It has been noted that endpoint events with different  $m_V$  or different  $\vec{U}_T$  generically have different slopes [51, 52, 53, 54, 55, 56].

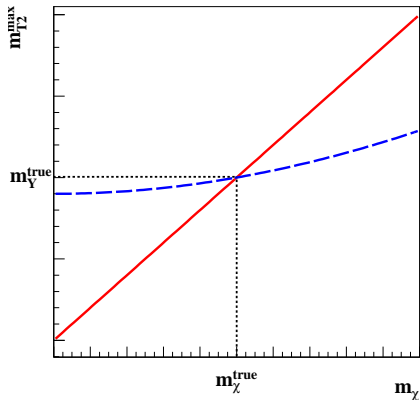


**Figure 2:** Pictorial representation of the  $m_{T2}$  curve for two events (solid vs. broken lines) in the endpoint region close to  $m_{T2}(m_\chi = m_\chi^{\text{true}}) = m_Y^{\text{true}}$ . The  $x$ - and  $y$ -axes are in arbitrary units.

This implies that the kink can be sharp enough to be visible if  $V$  corresponds to multi-particle states with wide range of  $m_V$  and/or if a large  $|\vec{U}_T|$  is available. As the possible range of  $m_V$  is bounded by  $m_Y^{\text{true}} - m_\chi^{\text{true}}$ , the kink can be sharp enough only when  $m_Y^{\text{true}}$  is substantially heavier than  $m_\chi^{\text{true}}$ . As for  $|\vec{U}_T|$ , although in principle it can be substantially larger than  $m_Y^{\text{true}}$ , in reality the best possible situation would be  $|\vec{U}_T| \sim m_Y^{\text{true}}$ .

### 2.3 Generalizations

Although  $\chi$  was identified as the LSP in the above discussion, the very same argument applies to the more general case where  $\chi$  is a generic SUSY particle produced by the decay of  $Y$  or  $\bar{Y}$ , as long as  $\chi(k)$  and  $\chi(l)$  have the same mass [61, 45]. For instance,  $\chi$  might be a heavier neutralino or a chargino, decaying into the LSP and some SM particles, provided one regards



all those particles as missing particles. Indeed, as already mentioned, in the following we will be applying the  $m_{T2}$ -kink method to gluino-pair decay in the scenarios of [10, 16], with  $\chi$  being a chargino or the second lightest neutralino respectively.<sup>4</sup> Looking at the SUSY spectra, summarized in table 1, the gluino undergoes a relatively short (2-step) cascade decay into  $\chi$  plus several visible particles, and also the gluino mass is sensibly above  $m_\chi$ . This by itself indicates that a visible kink might be possible even with events having a negligible  $|\vec{U}_T|$ .

In cases where the visible decay products involve multiple jets, it is often difficult to identify the endpoint position because of the smearing caused by poor jet momentum resolution. In such cases, to reduce the endpoint smearing, one can consider an alternative form of  $m_{T2}$  defined *solely* in terms of the jet *transverse* momenta [51, 54]:

$$m_{T2} = \min_{\vec{k}_T + \vec{l}_T = \vec{p}_T} \left[ \max \left( m_T(Y \rightarrow V_1 + \chi), m_T(\bar{Y} \rightarrow V_2 + \chi) \right) \right], \quad (2.8)$$

where now  $m_T(Y \rightarrow V + \chi)$  is given by

$$m_T^2 = m_{TV}^2 + m_\chi^2 + 2 \left( \sqrt{m_{TV}^2 + |\vec{p}_T|^2} \sqrt{m_\chi^2 + |\vec{k}_T|^2} - \vec{p}_T \cdot \vec{k}_T \right). \quad (2.9)$$

Here

$$m_{TV}^2(Y \rightarrow V + \chi) = \sum_\alpha m_\alpha^2 + 2 \sum_{\alpha > \beta} (E_{\alpha T} E_{\beta T} - \vec{p}_{\alpha T} \cdot \vec{p}_{\beta T}), \quad (2.10)$$

where  $\vec{p}_{\alpha T}$  is the measured transverse momentum of the  $\alpha$ -th jet in the set of visible decay products  $V$ , and  $E_{\alpha T} = \sqrt{m_\alpha^2 + |\vec{p}_{\alpha T}|^2}$ , with  $m_\alpha$  denoting the  $\alpha$ -th *parton* mass, rather than the jet invariant mass, i.e.  $m_\alpha = 0$  for non- $b$  jets and  $m_\alpha = m_b$  for  $b$ -tagged jets. As the transverse momentum can be measured with better accuracy than the other components, the  $m_{T2}$  defined in this way suffers less from jet momentum uncertainty. In addition, it still obeys all the features for a kink at  $m_\chi = m_\chi^{\text{true}}$  with  $m_{T2}^{\text{max}}(m_\chi = m_\chi^{\text{true}}) = m_Y$  at partonic level. On the other hand, as  $m_{TV} \leq m_V$ , the  $m_{T2}$  defined with the transverse mass  $m_{TV}$  has generically smaller statistics near the endpoint than the  $m_{T2}$  defined with the full invariant mass  $m_V$ . Previous studies suggest that the reduced statistics is not a severe drawback compared to the gain from reduced smearing [51, 54], and thus the  $m_{T2}$  defined in terms of the jet transverse momenta can reveal a kink even when the kink of  $m_{T2}$  defined with  $m_V$  is smeared away due to poor jet momentum resolution. In the following analysis including detector effects, we will use the  $m_{T2}$  defined with  $m_V$  if its distribution shows a clear endpoint, and the  $m_{T2}$  defined with  $m_{TV}$  otherwise.

To conclude this section, we would like to mention that several new methods of mass measurement for events involving invisible particles have recently been proposed, e.g. one exploiting the cusp structure of the distribution of certain kinematic variables [64] and another based on a generic algebraic singularity that arises in the observable phase space obtained by projecting out the unmeasurable kinematic variables [65]. It would be worthwhile to investigate how much useful those methods may be for the specific SUSY scenarios of [10, 16] that we are studying in this paper.

<sup>4</sup>One can further generalize  $m_{T2}$  to the case in which the parent or daughter particles are not identical [62, 63].

<b>SUSY production cross sections</b>				
	HS scenario		LS scenario	
	14 TeV	10 TeV	14 TeV	10 TeV
total (pb)	41	17	137	57
$\tilde{\chi}_1^\pm \tilde{\chi}_1^\mp$ (%)	12.7	18.7	5.7	8.7
$\tilde{\chi}_2^0 \tilde{\chi}_1^\pm$ (%)	24.7	36.6	11.2	17.1
$q\bar{q} \rightarrow \tilde{g}\tilde{g}$ (%)	9.1	9.7	5.1	6.1
$gg \rightarrow \tilde{g}\tilde{g}$ (%)	53.4	34.9	39.7	28.9
$gg \rightarrow \tilde{t}_1 \tilde{t}_1^*$ (%)	0.04	0.02	35.2	35.1
$f\bar{f} \rightarrow \tilde{t}_1 \tilde{t}_1^*$ (%)	0.02	0.01	3.0	4.1

**Table 2:** SUSY production cross sections from Pythia 6.42. Decay tables are calculated with SUSYHIT and then fed to Pythia. Missing entries are meant to be below 0.1 permil.

### 3. Strategy

In this section we apply the idea of  $m_{T2}$ -kink described above to the SUSY GUT scenarios exemplified in table 1, and henceforth referred to as HS (heavy stop) scenario (ref. [10]) and LS (light stop) scenario (ref. [16]), because of the heavy and respectively light stop relatively to each other. A first necessary piece of information is that of the main SUSY production cross sections for the two scenarios. Table 2 shows the most important production mechanisms, for  $pp$  events with  $\sqrt{s}$  equal to 10 or 14 TeV.<sup>5</sup> They have been calculated with Pythia 6.42 [66]. For both HS and LS scenarios the dominant SUSY-production mechanism is  $\tilde{g}\tilde{g}$ . Interestingly, for the LS scenario,  $\tilde{t}_1\tilde{t}_1^*$  production is also large, close to 40%. Finally, also  $\tilde{\chi}_2^0\tilde{\chi}_1^\pm$  associated production is non-negligible in both scenarios. The second needed piece of information is that of the main decay modes for the produced particles. These decay modes are reported in table 3, and calculated with SUSYHIT [67]. We will elaborate on these production and decay figures in due course during the analysis.

In the light of the information in tables 2 and 3, the rest of this section is devoted to a short description of our mass-determination procedure, as it would be carried out in a parton-level analysis. In order to provide a quick overview of the various steps, the full procedure is also schematically reported in table 4. This table shows that our procedure is able to determine the  $\tilde{g}$ ,  $\tilde{\chi}_1^0$ ,  $\tilde{\chi}_2^0$ ,  $\tilde{\chi}_1^\pm$  masses in either scenario and, for the LS scenario, also the  $\tilde{t}_1$  mass. The concrete implementation of our strategy, carried out on 100/fb of LHC data at the design center-of-mass energy of 14 TeV, and including realistic detector effects, is postponed to section 4.

#### 3.1 Strategy: LS scenario

Given the generally lighter masses and the higher cross sections for the LS scenario, our

<sup>5</sup>Our analysis will be focused on the 14 TeV case. The 10 TeV case is reported for guidance, with the aim of showing that production cross sections for all considered processes are such that our strategy should still apply at this value of  $\sqrt{s}$ .

Main decay modes (%)		
	HS scenario	LS scenario
$\Gamma_{\tilde{g}}$ (GeV)	$1.6 \cdot 10^{-5}$	3.3
$\tilde{g} \rightarrow \tilde{\chi}_2^0 g$	0.9	–
$\tilde{g} \rightarrow \tilde{\chi}_2^0 b\bar{b}$	41.7	–
$\tilde{g} \rightarrow \tilde{\chi}_2^0 q\bar{q}$ ( $q = u, d, s, c$ )	0.5	–
$\tilde{g} \rightarrow \tilde{\chi}_1^0 t\bar{t}$	20.1	–
$\tilde{g} \rightarrow \tilde{\chi}_1^0 b\bar{b}$	3.6	–
$\tilde{g} \rightarrow \tilde{\chi}_1^\pm t b$	31.5	–
$\tilde{g} \rightarrow \tilde{t}_1^{(*)} t$	–	100
$\Gamma_{\tilde{t}_1}$ (GeV)	25	$3.5 \cdot 10^{-3}$
$\tilde{t}_1 \rightarrow \tilde{g} t$	93.4	–
$\tilde{t}_1 \rightarrow \tilde{\chi}_1^0 t$	5.8	–
$\tilde{t}_1 \rightarrow \tilde{\chi}_1^+ b$	0.6	100
$\Gamma_{\tilde{\chi}_2^0}$ (GeV)	$8.2 \cdot 10^{-11}$	$2.6 \cdot 10^{-10}$
$\tilde{\chi}_2^0 \rightarrow \tilde{\chi}_1^0 \gamma$	62.2	94.6
$\tilde{\chi}_2^0 \rightarrow \tilde{\chi}_1^0 b\bar{b}$	31.5	0.8
$\tilde{\chi}_2^0 \rightarrow \tilde{\chi}_1^0 \ell^+ \ell^-$ ( $\ell = e, \mu$ )	0.7	1.0
$\tilde{\chi}_2^0 \rightarrow \tilde{\chi}_1^0 \tau^+ \tau^-$	1.8	0.9
$\Gamma_{\tilde{\chi}_1^\pm}$ (GeV)	$1.8 \cdot 10^{-11}$	$1.2 \cdot 10^{-11}$
$\tilde{\chi}_1^\pm \rightarrow \tilde{\chi}_1^0 \tau \nu_\tau$	91.0	39.5
$\tilde{\chi}_1^\pm \rightarrow \tilde{\chi}_1^0 \ell \nu_\ell$ ( $\ell = e, \mu$ )	4.7	42.7
$\tilde{\chi}_1^\pm \rightarrow \tilde{\chi}_1^0 u d / c s$	4.3	17.8

**Table 3:** Main decay modes in % for  $\tilde{g}$ ,  $\tilde{t}_1$ ,  $\tilde{\chi}_2^0$  and  $\tilde{\chi}_1^\pm$ , calculated with SUSYHIT.

strategy is richer in this case, and we describe it first.

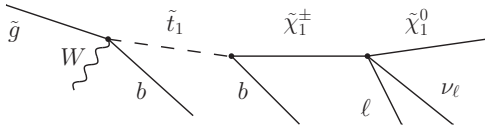


**Figure 3:** Decay chain of interest for step 1 (LS scenario).

$qq' \tilde{\chi}_1^0$  would have the advantage that all the decay products apart from the  $\tilde{\chi}_1^0$  would be reconstructible, *in principle*. However, in practice, the event trigger would consist of 2  $b$  jets and 4 additional non- $b$  jets (2 jets from  $W$  and another 2 jets from  $\tilde{\chi}_1^\pm$ ) for *each* of the two decay chains, making this channel very challenging already on account of the jet combinatoric error.

A more promising strategy is to focus instead on leptonically-decaying charginos, namely  $\tilde{\chi}_1^\pm \rightarrow \tilde{\chi}_1^0 \ell \nu_\ell$ , and to regard the whole  $\tilde{\chi}_1^\pm$ -initiated decay chain (see fig. 3) as

**Step 1:** Construct  $m_{T2}$  for  $\tilde{g}\tilde{g} \rightarrow 4 b + 2 W (+ 2 \ell) + \cancel{p}_T$  decay events, thereby measuring  $m_{\tilde{g}}$  and  $m_{\tilde{\chi}_1^\pm}$

In the scenario of ref. [16], the gluino decays always as  $\tilde{g} \rightarrow \tilde{t}_1 t$ , with the top quark subsequently decaying as  $t \rightarrow bW$  and the  $\tilde{t}_1$  as  $\tilde{\chi}_1^\pm b$ . Requiring the  $\tilde{\chi}_1^\pm$  to decay as

	Step	Event trigger	Event variable	Allows to determine
LS scenario	1	$\tilde{g}\tilde{g} \rightarrow 4b + 2W (+2\ell) + \cancel{p}_T$	$m_{T2}$ (with $2\ell \in \cancel{p}_T$ )	$m_{\tilde{g}}$ and $m_{\tilde{\chi}_1^\pm}$
	2	$\tilde{t}_1\tilde{t}_1 \rightarrow 2b + 4q + \cancel{p}_T$	$m_{T,bqq}$	$m_{\tilde{t}_1} - m_{\tilde{\chi}_1^0}$
	"	"	$m_{T,qq}$	$m_{\tilde{\chi}_1^\pm} - m_{\tilde{\chi}_1^0}$
	3	$\tilde{\chi}_1^\pm\tilde{\chi}_2^0 \rightarrow \ell^+\ell^-\ell' + \cancel{p}_T$	$m_{\ell\ell}$	$m_{\tilde{\chi}_2^0} - m_{\tilde{\chi}_1^0}$
HS scenario	1	$\tilde{g}\tilde{g} \rightarrow 4b (+2\gamma) + \cancel{p}_T$	$m_{T2}$ (with $2\gamma \in \cancel{p}_T$ )	$m_{\tilde{g}}$ and $m_{\tilde{\chi}_2^0}$
	2	$\tilde{\chi}_1^\pm\tilde{\chi}_2^0 \rightarrow \ell^+\ell^- + \ell' + \cancel{p}_T$	$m_{\ell\ell}$	$m_{\tilde{\chi}_2^0} - m_{\tilde{\chi}_1^0}$
	3	$\tilde{\chi}_1^\pm\tilde{\chi}_2^0 \rightarrow 2q + 2\ell + \cancel{p}_T$	$m_{qq}$	$m_{\tilde{\chi}_1^\pm} - m_{\tilde{\chi}_1^0}$
	"	"	$m_{\ell\ell}$	$m_{\tilde{\chi}_2^0} - m_{\tilde{\chi}_1^0}$

**Table 4:** Overview of our mass-determination strategy.

$\cancel{p}_T$ . In this case the final state will contain  $2b + W + \ell\nu_\ell + \tilde{\chi}_1^0$  for each decay chain, with  $\ell$  either of  $e, \mu$ . The  $\cancel{p}_T$  will then be the sum of the transverse momenta of the  $\tilde{\chi}_1^0$  and of the  $\ell\nu$  pair. Concerning the  $W$ , one can require it to decay in a  $qq'$  pair, so that  $m_{qq} = m_W$  (up to the  $W$  width) in each of the two decay chains. The event topology to look at is therefore  $4b + 2W + 2\ell + \cancel{p}_T$ : while the combinatoric problem has not completely disappeared, it has been substantially mildened with respect to the case mentioned in the previous paragraph.

Constructing the  $m_{T2}$ -kink for this event topology (with, as mentioned, the 2 leptons'  $p_T$  included in  $\cancel{p}_T$ ) allows to determine simultaneously  $m_{\tilde{g}}$  and  $m_{\tilde{\chi}_1^\pm}$ .

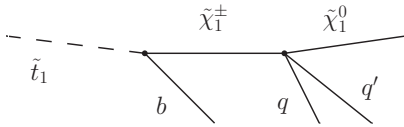


**Figure 4:** Decay chain of interest for step 2 (LS scenario).

can further require the  $\tilde{\chi}_1^\pm$  to decay (besides the invisible  $\tilde{\chi}_1^0$ ) into visible products (see fig. 4), which happens in about 20% of the cases. The mass differences  $m_{\tilde{t}_1} - m_{\tilde{\chi}_1^0}$  and  $m_{\tilde{\chi}_1^\pm} - m_{\tilde{\chi}_1^0}$  can then be obtained as the endpoints of the transverse-mass distributions calculated respectively on the  $bqq'$  and  $qq'$  systems, for each of the two decay chains of the event. An evident problem here is to correctly assign the  $b$ - and  $q$ -jets to the two decay chains. We will come back to this in the analysis.

**Step 2:** For  $\tilde{t}_1\tilde{t}_1 \rightarrow 2b + 4q + \cancel{p}_T$  events, determine the mass differences  $m_{\tilde{t}_1} - m_{\tilde{\chi}_1^0}$  and  $m_{\tilde{\chi}_1^\pm} - m_{\tilde{\chi}_1^0}$  from the endpoints of the transverse-mass distributions  $m_{T,bqq}$  and  $m_{T,qq}$ , respectively

In the scenario of ref. [16], given the lightness of the  $\tilde{t}_1$ , its pair-production is substantial and the only kinematically allowed decay mode is  $\tilde{t}_1 \rightarrow \tilde{\chi}_1^\pm b$ . One

**Step 3:** For  $\tilde{\chi}_1^\pm\tilde{\chi}_2^0 \rightarrow \ell^+\ell^- + \ell' + \cancel{p}_T$  events, determine the mass difference  $m_{\tilde{\chi}_2^0} - m_{\tilde{\chi}_1^0}$  from the endpoint of the invariant-mass distribution  $m_{\ell\ell}$

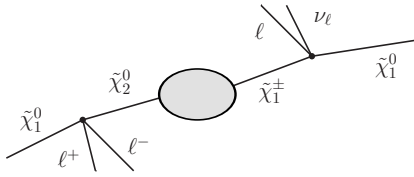


**Figure 5:** Decay chain of interest for step 3 (LS scenario).

$m_{\tilde{\chi}_2^0}$ , since the lightest neutralino mass is already known from the previous step 2.

### 3.2 Strategy: HS scenario

We next turn to discussing SUSY mass determinations within the HS scenario of table 1.

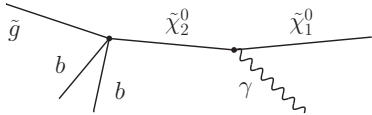


**Figure 6:** Decay chain of interest for step 1 (HS scenario).

**Step 1:** Construct the  $m_{T2}$  variable for  $\tilde{g}\tilde{g} \rightarrow 4b (+ 2\gamma) + \cancel{p}_T$  decay events, thereby measuring  $m_{\tilde{g}}$  and  $m_{\tilde{\chi}_2^0}$

Gluino-gluino production, followed by gluino decaying as  $\tilde{g} \rightarrow b\bar{b}\tilde{\chi}_2^0$ , is probably the golden mode for the HS scenario. If one further considers the radiative decay of the  $\tilde{\chi}_2^0$  into  $\tilde{\chi}_1^0$  (note that this decay mode has the largest branching ratio), the implied event trigger, namely  $4b + 2\gamma + \cancel{p}_T$ , has very small contamination from SM background. Including the gammas in the  $\cancel{p}_T$ , the kink in the  $m_{T2}$  variable constructed for these events allows to simultaneously determine  $m_{\tilde{g}}$  and  $m_{\tilde{\chi}_2^0}$ .

Alternatively, one might attempt to apply the  $m_{T2}$ -kink method to the subsystem involving  $2\tilde{\chi}_2^0$  as parent particles and  $2\gamma$  as their visible decay products. In this case, the kink in  $m_{T2}$  arises due to nonzero upstream transverse momentum and it allows to determine the masses of  $\tilde{\chi}_2^0$  and  $\tilde{\chi}_1^0$ . From the analysis we find however that the resulting kink is not as clean as the one obtained in the approach of the previous paragraph, where also the  $4b$  are included as visible decay products.

**Step 2:** For  $\tilde{\chi}_1^\pm \tilde{\chi}_2^0 \rightarrow \ell^+ \ell^- + \ell' + \cancel{p}_T$  events, determine the mass difference  $m_{\tilde{\chi}_2^0} - m_{\tilde{\chi}_1^0}$  from the endpoint of the invariant-mass distribution  $m_{\ell\ell}$

The implementation of this step is entirely analogous as in step 3 of the LS scenario.

**Step 3:** For  $\tilde{\chi}_1^\pm \tilde{\chi}_2^0 \rightarrow 2q + 2\ell + \cancel{p}_T$  events, determine the mass difference  $m_{\tilde{\chi}_1^\pm} - m_{\tilde{\chi}_1^0}$  from the endpoint of the invariant-mass distribution  $m_{qq}$  (and again  $m_{\tilde{\chi}_2^0} - m_{\tilde{\chi}_1^0}$  from  $m_{\ell\ell}$ )

Still to be determined is the  $\tilde{\chi}_1^\pm$  mass. At variance with the LS scenario, this information cannot be easily extracted from secondary  $\tilde{\chi}_1^\pm$  generated in  $\tilde{g}\tilde{g}$  or  $\tilde{t}_1\tilde{t}_1$  production events. However, one can consider  $\tilde{\chi}_1^\pm \tilde{\chi}_2^0$  associated production, with the  $\tilde{\chi}_1^\pm$  decaying as  $\tilde{\chi}_1^\pm \rightarrow \tilde{\chi}_1^0 qq'$ . Concerning the  $\tilde{\chi}_2^0$ , the radiative decay to  $\tilde{\chi}_1^0$  is, as already noted above, the one with the largest branching ratio. However, the resulting event topology, namely  $2q + \gamma$

+  $\cancel{p}_T$ , is dominated by background events, that we were not able to get rid of. For this reason, we required the  $\tilde{\chi}_2^0$  to decay as  $\tilde{\chi}_1^0 \ell \ell$  (and veto on  $\ell = \tau$ , since its decay would produce missing momentum from neutrinos). The invariant-mass distribution of the  $qq'$  pair is bounded from above by  $m_{\tilde{\chi}_1^\pm} - m_{\tilde{\chi}_1^0}$ , allowing to obtain  $m_{\tilde{\chi}_1^\pm}$ , since  $m_{\tilde{\chi}_1^0}$  is known from step 1.

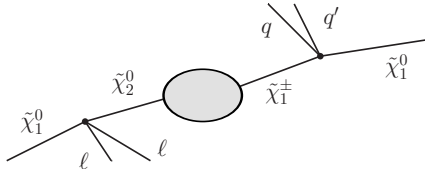


**Figure 7:** Decay chain of interest for step 3 (HS scenario).

In addition, the invariant-mass distribution  $m_{\ell\ell}$  provides a cross-check with step 2 on the determination of  $m_{\tilde{\chi}_2^0} - m_{\tilde{\chi}_1^0}$ .

## 4. Analysis and results

In this section we would like to show that the mass-determination strategy described in the previous section is indeed practicable with real data collected at the Atlas [44] and CMS [68] experiments, and permits to determine most of the considered masses within about 20 GeV of the true values, with an integrated luminosity not exceeding  $100 \text{ fb}^{-1}$  at the design LHC center-of-mass energy of 14 TeV. To address this point, we have simulated full events with Pythia 6.42 [66] and modeled LHC detector effects with PGS4 [69]. Specifically, we adopted the default `lhcb.par` card that comes with the latest PGS4 version. Purpose of this analysis is to get a presumably realistic idea of how much do the signals degrade once detector effects are taken into account. It goes without saying that the ‘true’ answer will require a full-fledged detector simulation, with insider knowledge of all acceptance and resolution details, which is prerogative of experimentalists only.

We next proceed to the discussion of the analysis, following the steps described in the previous section.

### 4.1 Analysis: LS scenario

**Step 1:** Construct  $m_{T2}$  for  $\tilde{g}\tilde{g} \rightarrow 4b + 2W (+ 2\ell) + \cancel{p}_T$  decay events, thereby measuring  $m_{\tilde{g}}$  and  $m_{\tilde{\chi}_1^\pm}$

We select events with 4 jets tagged as  $b$ ,<sup>6</sup> 4  $q$  jets (here and henceforth, we will so indicate jets not tagged as  $b$ ) and 2 leptons. To reconstruct the  $W$  bosons, we make all the possible di-jet combinations out of the 4  $q$  jets, and accept only events for which *both* di-jet invariant masses for at least one pairing are within  $M_W \pm 20$  GeV. In case that more than one pairing fulfill this requirement, we choose the pairing with minimal  $\sqrt{\Delta M_W^2(2q) + \Delta M_W^2(2q')}$ . Furthermore, in order to eliminate possible SM backgrounds, we impose the following cuts:

- (a)  $p_{T1,2,3,4} > 50, 30, 20, 20$  GeV for the 4  $b$  jets;
- (b) Missing transverse energy  $\cancel{E}_T > 50$  GeV;

<sup>6</sup>For the sake of clarity, the  $b$ -tagging algorithm adopted in our analysis is the one defined as ‘loose tagging’ in PGS [69]. Needless to say, a fully rigorous treatment of this issue requires a dedicated experimental analysis.

(c) Transverse sphericity  $S_T > 0.15$ .<sup>7</sup>

As this process involves several jets, in order to reduce the uncertainty associated with jet momentum resolution we use here the  $m_{T2}$  defined in terms of the total transverse mass,  $m_{TV}$ , of the 4 jets in the gluino decay  $\tilde{g} \rightarrow t\bar{t}_1 \rightarrow bqqb\tilde{\chi}_1^\pm$ , see eq. (2.10). Furthermore, in the procedure to compute  $m_{TV}$ , we do not use the invariant mass of each jet recorded in the detector, but simply set  $m_j = 0$  for non- $b$  jets, and  $m_j = m_b$  for  $b$ -tagged jets. This means that, for a given trial chargino mass, only the jet transverse momenta are used for the calculation of  $m_{T2}$ . Quite often, this approach turns out to be useful for identifying the endpoint when the decay product of each mother particle involves more than one (or two) jets. Still, the calculation of  $m_{T2}$  is subject to combinatoric uncertainty due to correctly pairing the 4  $b$  jets with the two reconstructed  $W$  bosons. To perform this pairing, we use the so-called  $m_{T\text{Gen}}$  pairing scheme [70].<sup>8</sup>

With the events passing the above selection criteria,<sup>9</sup> we have constructed the  $m_{T2}(m_\chi)$  distribution, with trial chargino mass  $m_\chi \in [0, 200]$  GeV. The resulting density plot is shown in fig. 8 (upper-left panel). The kink structure can be roughly located by inspecting the uppermost dark lines (indicating the largest density of events), if one neglects the more sparse (lighter in color) contributions from background events.

A quantitative determination of the  $m_{T2}$  maximum line can be carried out as follows. First, one fits the endpoint of the  $m_{T2}$  distributions obtained at fixed  $m_\chi$ . Examples of these distributions, and their endpoint fits to a two-segments line, are reported in fig. 8 (lower panels) for the values  $m_\chi = \{0, 100, 197\}$  GeV. Here and henceforth (figs. 8-11), the two-segments line is parameterized as

$$\begin{aligned} y &= p_1(x - p_0) + p_2x + p_3, & \text{for } x < p_0, \\ y &= p_2x + p_3, & \text{for } x > p_0. \end{aligned} \quad (4.2)$$

The resulting endpoint values of  $m_{T2}$  for the various values of  $m_\chi$ , namely  $m_{T2}^{\text{max}}(m_\chi)$ , are shown in fig. 8 (upper-right panel), with bars representing the statistical error. To identify the kink position, we then fit those endpoint values with appropriate fitting functions.

---

<sup>7</sup>We adopt the same definition as [44], namely

$$S_T \equiv \frac{2\lambda_2}{\lambda_1 + \lambda_2}, \quad (4.1)$$

where  $\lambda_{1,2}$  are the eigenvalues of the  $2 \times 2$  sphericity tensor  $S_{ij} = \sum_k p_i^k p_j^k$ , with  $k$  running on all the visible particles, and  $i, j = \{1, 2\}$  labeling the momentum transverse component. SUSY events tend to be spherical ( $S_T \sim 1$ ) as opposed to back-to-back.

<sup>8</sup>In the present example, the  $m_{T\text{Gen}}$  scheme works as follows. Assuming that only one of the (three) di-jet pairings among  $q$  jets fulfills the  $M_W$  requirement, there are still six possible ways of forming two  $b$  di-jets and of assigning them to the two reconstructed  $W$  bosons. For each of these combinations, we calculate the  $m_{T2}(m_\chi)$  value for fixed  $m_\chi$ , and pick the combination corresponding to the minimum  $m_{T2}(m_\chi)$ . As  $m_\chi$  value we took 100 GeV and we checked that the pairing choice does not change when reasonably varying  $m_\chi$ .

<sup>9</sup>In particular, we checked by a parton-level analysis that the adopted  $m_{T\text{Gen}}$  pairing scheme is effective in reducing the jet combinatoric error, while not significantly affecting the final  $m_{T2}$  distribution with respect to the true pairing.

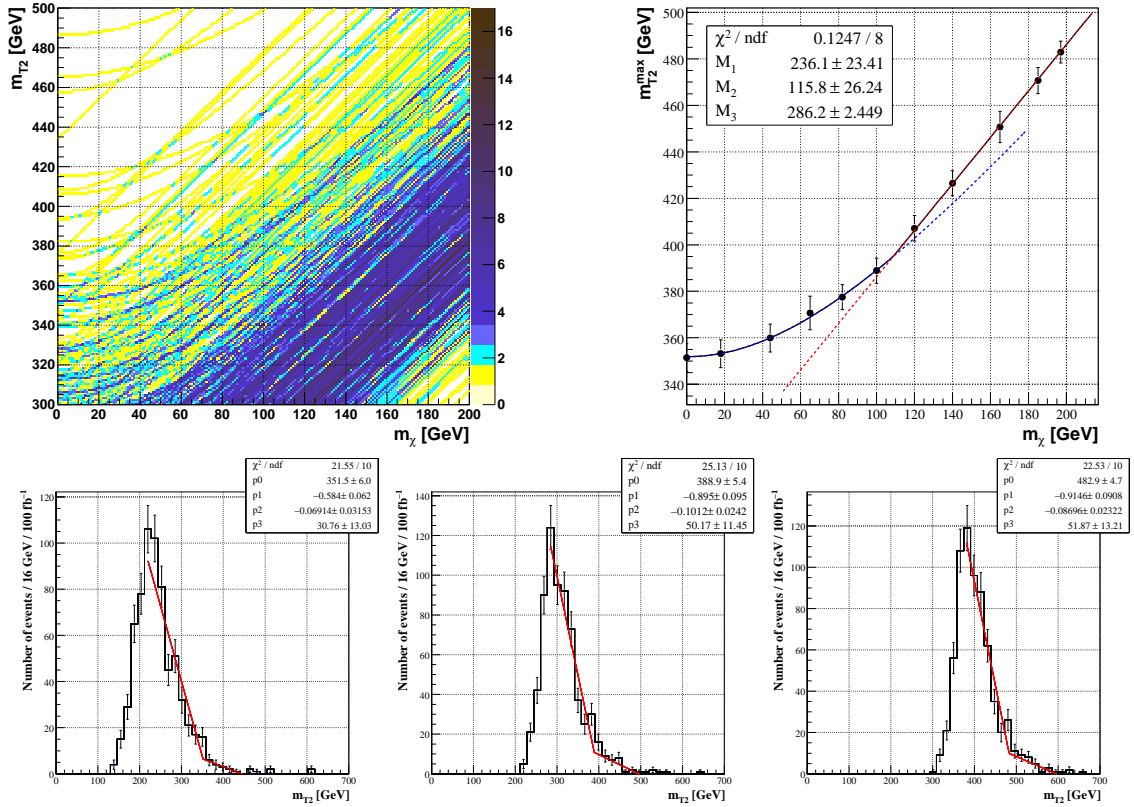


**Figure 8:** *Upper-left panel:*  $m_{T2}(m_\chi)$  density plot for the events of step 1, LS scenario. The color code on the right of the plot represents the number of events described by each line; *Upper-right panel:* fit to the corresponding maximum  $m_{T2}(m_\chi)$ ; *Lower panels:*  $m_{T2}$  distribution for the events of step 1, LS scenario, with  $m_\chi = \{0, 100, 197\}$  GeV.

To this end, one can use the known analytic form of  $m_{T2}(m_\chi)$  [51, 54] for events with  $m_{T2}(m_\chi = m_{\tilde{\chi}_1^\pm}) = m_{\tilde{g}}$  and negligible upstream transverse momentum:

$$m_{T2}(m_\chi, m_V) = \frac{m_{\tilde{g}}^2 - m_{\tilde{\chi}_1^\pm}^2 + m_V^2}{2m_{\tilde{g}}} + \frac{\sqrt{(m_{\tilde{g}}^2 + m_{\tilde{\chi}_1^\pm}^2 - m_V^2)^2 + 4m_{\tilde{g}}^2(m_\chi^2 - m_{\tilde{\chi}_1^\pm}^2)}}{2m_{\tilde{g}}}, \quad (4.3)$$

where  $m_V$  denotes the total invariant (or transverse) mass of the  $2b + 2q$  jets in the gluino decay. From this  $m_{T2}$  functional form, one can easily notice that  $m_{T2}^{\max} = m_{T2}(m_V = m_V^{\max})$  for  $m_\chi > m_{\tilde{\chi}_1^\pm}$ , while  $m_{T2}^{\max} = m_{T2}(m_V = m_V^{\min})$  for  $m_\chi < m_{\tilde{\chi}_1^\pm}$ , hence  $m_{T2}^{\max}$  shows a kink at  $m_\chi = m_{\tilde{\chi}_1^\pm}$ . Generically,  $m_V^{\max} \leq m_{\tilde{g}} - m_{\tilde{\chi}_1^\pm}$  and  $m_V^{\min} \geq 0$ , and one easily finds  $m_{T2}^{\max} = m_{\tilde{g}} - m_{\tilde{\chi}_1^\pm} + m_\chi$  for  $m_V^{\max} = m_{\tilde{g}} - m_{\tilde{\chi}_1^\pm}$ .

The  $m_{T2}$  endpoint values in fig. 8 for  $m_\chi > m_{\tilde{\chi}_1^\pm}$  indicate that they can be well described by a straight line, implying that  $m_V^{\max}$  is close to  $m_{\tilde{g}} - m_{\tilde{\chi}_1^\pm}$ . Inspired by the



analytic form (4.3), we then use the following fitting functions to find the kink position:

$$\begin{aligned} m_{T2}^{\max} &= M_1 + \sqrt{M_2^2 + m_\chi^2} && \text{if } m_\chi < m_{\tilde{\chi}_1^\pm}, \\ m_{T2}^{\max} &= M_3 + m_\chi && \text{if } m_\chi > m_{\tilde{\chi}_1^\pm}, \end{aligned} \quad (4.4)$$

where  $M_i$  ( $i = 1, 2, 3$ ) are fitting parameters. The best-fit curves are shown in fig. 8 (upper-right panel), together with the corresponding values of  $M_i$ . The resulting gluino and chargino masses are given by  $m_{\tilde{\chi}_1^\pm} = 109(17)$  GeV and  $m_{\tilde{g}} = 395(16)$  GeV, which are fully compatible with the true values in table 1. We also find that the  $m_{T2}^{\max}$ -curves in fig. 8, which describe data at detector level, are reasonably close to the curves obtained at parton level.

**Step 2:** For  $\tilde{t}_1\tilde{t}_1 \rightarrow 2b + 4q + \cancel{p}_T$  events, determine the mass differences  $m_{\tilde{t}_1} - m_{\tilde{\chi}_1^0}$  and  $m_{\tilde{\chi}_1^\pm} - m_{\tilde{\chi}_1^0}$  from the endpoints of the transverse-mass distributions  $m_{T,bqq}$  and  $m_{T,qq}$ , respectively

To select these events, we need to require 2 jets tagged as  $b$ , 4  $q$  jets, and no leptons. The channel of  $\tilde{t}_1$  pair production is subject to SM backgrounds coming mostly from  $t\bar{t}$  or  $WW + 2b$  production. These backgrounds can be eliminated efficiently by the following selection cuts

- (a)  $p_{T1,2} > 50, 25$  GeV on the 2  $b$  jets;
- (b)  $p_{T1,2,3,4} > 50, 25, 20, 10$  GeV on the 4  $q$  jets;
- (c)  $\cancel{E}_T > 100$  GeV;
- (d) Transverse sphericity  $S_T > 0.15$ .

For the events passing the above cuts (a)-(d), we calculated, event by event, all possible di-jet transverse mass values out of the 4  $q$  jets and picked the minimum value among them. Here we use the di-jet transverse mass  $m_{T,jj}$ , rather than the di-jet invariant mass  $m_{jj}$ , as the endpoint of  $m_{jj}$  is severely smeared. The corresponding distribution is shown in fig. 9 (upper-left panel). Fitting the endpoint region to a two-segments line, we obtain  $m_{T,jj}^{\max} = m_{\tilde{\chi}_1^\pm} - m_{\tilde{\chi}_1^0} = 51.8(1.7)$  GeV, corresponding to  $m_{\tilde{\chi}_1^0} \approx 58$  GeV, a good estimate of the true value in table 1. A completely analogous procedure can be adopted for the transverse mass of the  $bqq'$  system, and the resulting distribution is shown in fig. 9 (upper-right panel). The fitted endpoint  $m_{T,bqq}^{\max}$  of this distribution allows to determine the  $\tilde{t}_1$  mass through the following formula

$$m_{\tilde{t}_1} = \sqrt{\frac{(m_{T,bqq}^{\max})^2 + m_{\tilde{\chi}_1^\pm}^2 - m_{\tilde{\chi}_1^0}^2}{1 - m_{\tilde{\chi}_1^0}^2/m_{\tilde{\chi}_1^\pm}^2}}, \quad (4.5)$$

implying  $m_{\tilde{t}_1} \approx 206$  GeV, again consistent with the true value in table 1.<sup>10</sup>

---

<sup>10</sup>Note that, if the relation  $m_{\tilde{\chi}_1^\pm}^2 = m_{\tilde{t}_1} m_{\tilde{\chi}_1^0}$  is fulfilled (as is our case within about  $(25 \text{ GeV})^2$ ), eq. (4.5) simplifies to  $m_{T,bqq}^{\max} = m_{\tilde{t}_1} - m_{\tilde{\chi}_1^0}$ .

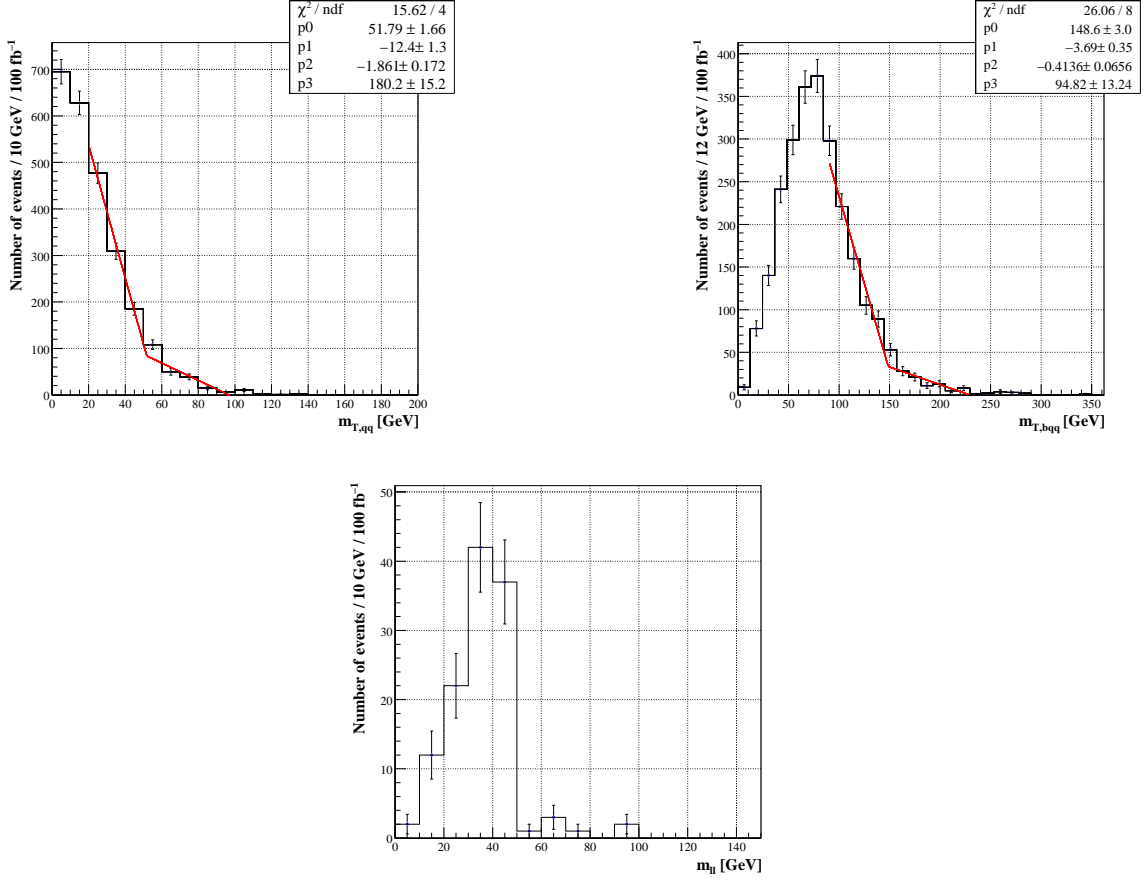


**Figure 9:** *Upper-left panel:* transverse mass distribution  $m_{T,qq}$  (step 2, LS scenario); *Upper-right panel:*  $bqq$ -jet transverse mass distribution (step 2, LS scenario); *Lower panel:* invariant mass distribution of the  $\ell^+\ell^-$  pair (step 3, LS scenario).

**Step 3:** For  $\tilde{\chi}_1^\pm \tilde{\chi}_2^0 \rightarrow \ell^+\ell^- + \ell' + \cancel{p}_T$  events, determine the mass difference  $m_{\tilde{\chi}_2^0} - m_{\tilde{\chi}_1^0}$  from the endpoint of the invariant-mass distribution  $m_{\ell\ell}$

To select these events, we require 2 leptons (either  $e$  or  $\mu$ ) of same flavor and opposite charge, one additional lepton of different flavor (with veto on hadronically decaying taus), and no jets. To clean up the event selection from possible backgrounds, we also impose the following cuts:

- (a)  $p_{T1,2} > 20, 15$  GeV on the 2 leptons of same flavor;
- (b)  $p_T > 15$  GeV on the lepton of different flavor;
- (c)  $\cancel{E}_T > 50$  GeV;
- (d) Transverse sphericity  $S_T > 0.15$ .

The invariant mass distribution constructed with the 2 leptons of same flavor is shown in fig. 9 (lower panel). The fact that, in general, the lepton signal is quite accurately

reconstructed explains the clear end point structure of the invariant mass distribution at 50 GeV (even with a limited number of events). This endpoint value is in agreement with the expected  $m_{\tilde{\chi}_2^0} - m_{\tilde{\chi}_1^0} \doteq 51$  GeV from table 1.

## 4.2 Analysis: HS scenario

**Step 1:** Construct the  $m_{T2}$  variable for  $\tilde{g}\tilde{g} \rightarrow 4 b (+ 2 \gamma) + \cancel{p}_T$  decay events, thereby measuring  $m_{\tilde{g}}$  and  $m_{\tilde{\chi}_2^0}$

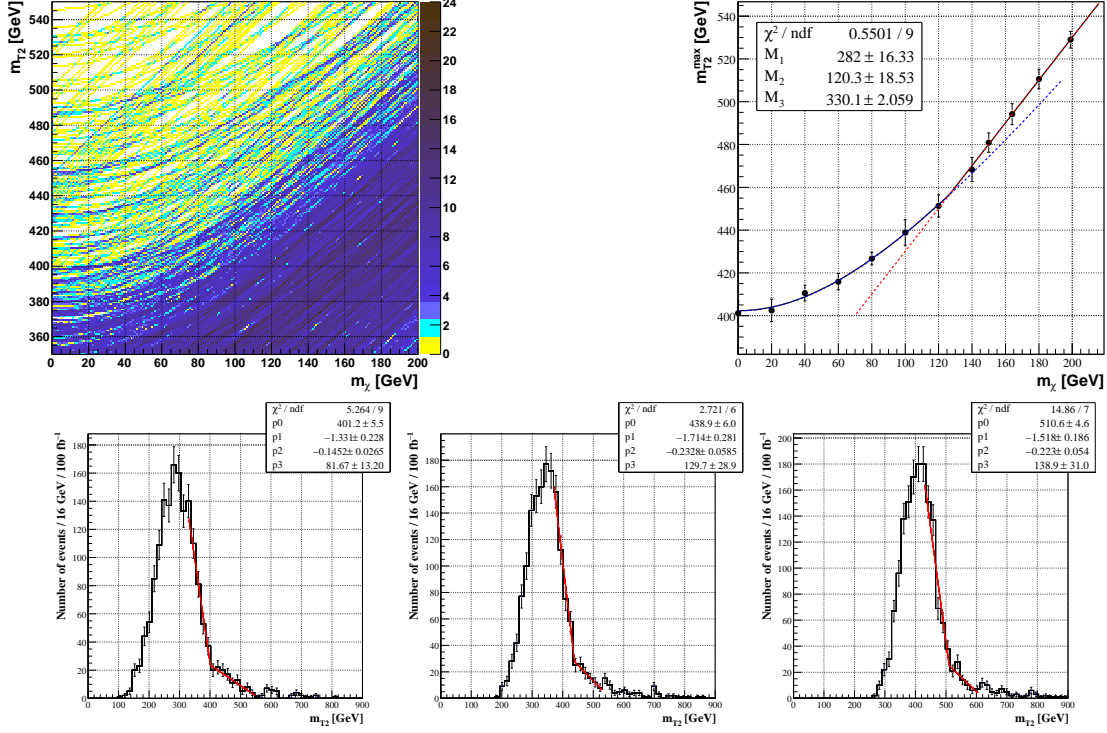


**Figure 10:** *Upper-left panel:*  $m_{T2}(m_\chi)$  density plot for the events of step 1, HS scenario. The color code on the right of the plot represents the number of events described by each line; *Upper-right panel:* fit to the corresponding maximum  $m_{T2}(m_\chi)$ ; *Lower panels:*  $m_{T2}$  distribution for the events of step 1, HS scenario, with  $m_\chi = \{0, 100, 180\}$  GeV.

Within  $\tilde{g}\tilde{g}$  production, the decay  $\tilde{g} \rightarrow \tilde{\chi}_2^0 b\bar{b}$ , followed by  $\tilde{\chi}_2^0 \rightarrow \tilde{\chi}_1^0 \gamma$  is the dominant channel. Since this channel is the only possible one giving 4 jets, 2  $\gamma$  and no lepton, it may not be necessary to require  $b$  tagging. Indeed, we select the above event content without  $b$  tagging. We however impose the following cuts as well:

- (a)  $p_{T1,2,3,4} > 120, 70, 30, 20$  GeV on the 4 jets;
- (b)  $p_{T1,2} > 50, 20$  GeV on the hard photons;

- (c)  $\cancel{E}_T > 100$  GeV;
- (d) Transverse sphericity  $S_T > 0.15$ .

On the selected events, we calculate  $m_{T2}(m_\chi)$  with the 4 jets according to the  $m_{T\text{Gen}}$  pairing scheme, and treating the 2  $\gamma$  as part of the  $\cancel{E}_T$ . Here we use the di-jet invariant mass  $m_{jj}$ , rather than the transverse mass, to compute  $m_{T2}$ , as the resulting  $m_{T2}$  distribution shows a reasonably clean endpoint structure.

The  $m_{T2}(m_\chi)$  density plot, displayed in fig. 10 (upper-left panel), shows a substantial number of spurious events contributing to the maximum  $m_{T2}$  line region, impairing a ‘by eye’ determination of the kink. Still, we can quantify the kink position by following the same strategy as step 1, LS scenario, namely fitting first the endpoint of the  $m_{T2}$  distributions obtained at fixed  $m_\chi$  values. Fig. 10 (lower panels) shows those distributions and fitted endpoints for  $m_\chi = \{0, 100, 180\}$ . Fitting those endpoints (obtained for various values of  $m_\chi$ ) to the function in eq. (4.4) (see fig. 10, upper-right panel), we get the kink position at  $m_{\tilde{\chi}_2^0} = 126(16)$  GeV and  $m_{\tilde{g}} = 456(15)$  GeV, which are in agreement with the true values in table 1. (The best-fit values of  $M_i$  are also reported in the figure.) Comparing to the parton level result, we find the kink to be not as sharp as expected. The main reason for this is that a large portion of the events with small  $m_{jj}$ , that provide the true  $m_{T2}^{\text{max}}$  for  $m_\chi < m_{\tilde{\chi}_2^0}$ , are eliminated by the selection cuts.

**Step 2:** For  $\tilde{\chi}_1^\pm \tilde{\chi}_2^0 \rightarrow \ell^+ \ell^- + \ell' + \cancel{p}_T$  events, determine the mass difference  $m_{\tilde{\chi}_2^0} - m_{\tilde{\chi}_1^0}$  from the endpoint of the invariant-mass distribution  $m_{\ell\ell}$

This step is completely analogous to step 3 of the LS scenario. We require two leptons ( $e$  or  $\mu$ ) of same flavor and opposite charge, one lepton of different flavor<sup>11</sup>, and no jets. To remove possible backgrounds, we also impose the following cuts:

- (a)  $p_{T1,2} > 20, 10$  GeV on the 2 leptons of same flavor;
- (b)  $p_T > 10$  GeV on the lepton of different flavor;
- (c)  $\cancel{E}_T > 50$  GeV.

The invariant mass distribution constructed with the 2 leptons of same flavor is shown in fig. 11 (upper-left panel). Again, the accuracy with which lepton signals are in general reconstructed explains the clear endpoint structure of the invariant mass distribution at 60 GeV. This endpoint agrees with the expected value  $m_{\tilde{\chi}_2^0} - m_{\tilde{\chi}_1^0} \doteq 59$  GeV from table 1.

**Step 3:** For  $\tilde{\chi}_1^\pm \tilde{\chi}_2^0 \rightarrow 2q + 2\ell + \cancel{p}_T$  events, determine the mass difference  $m_{\tilde{\chi}_1^\pm} - m_{\tilde{\chi}_1^0}$  from the endpoint of the invariant-mass distribution  $m_{qq}$  (and again  $m_{\tilde{\chi}_2^0} - m_{\tilde{\chi}_1^0}$  from  $m_{\ell\ell}$ )

We select these events by requiring 2  $q$  jets and 2 leptons ( $e$  or  $\mu$ ) of same flavor and opposite charge. We also impose the following cuts :

---

<sup>11</sup>At variance with step 3 of the LS scenario, here we also allow this one lepton to be a hadronically decaying tau in order to have larger statistics.

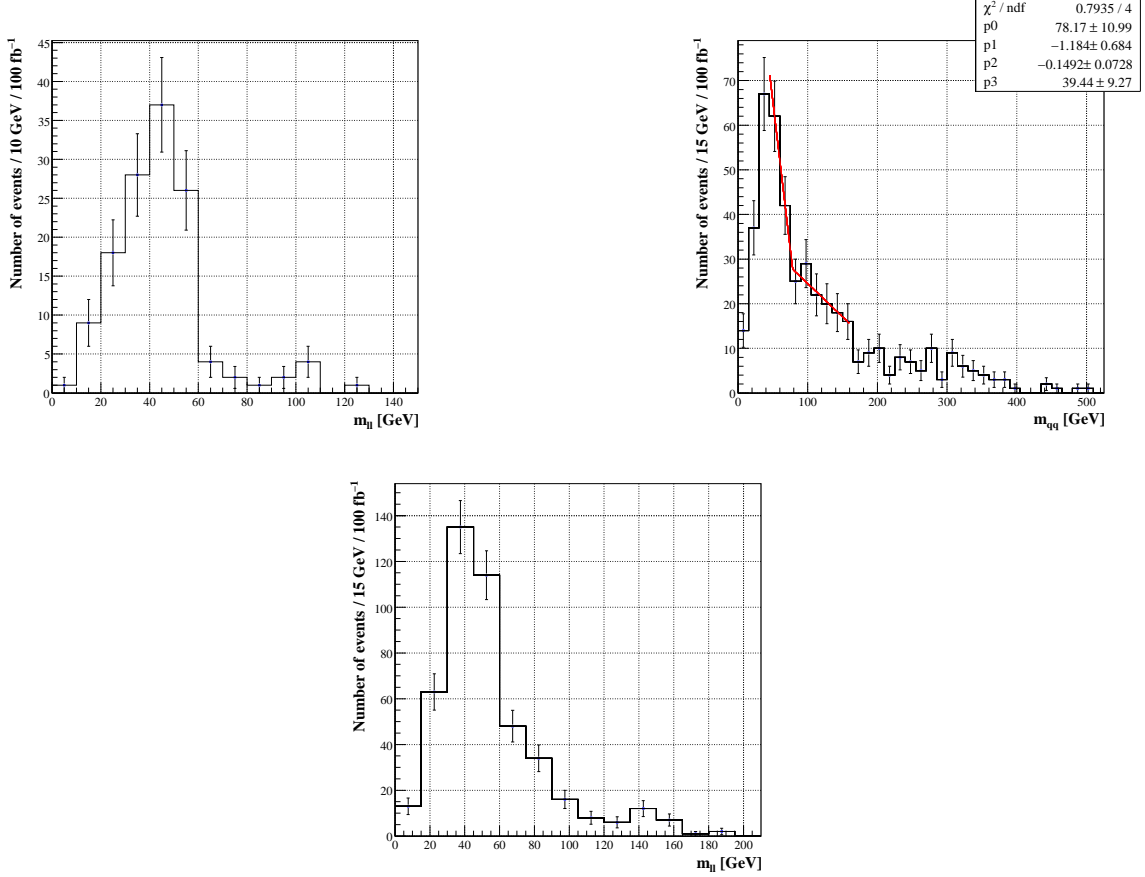


**Figure 11:** *Upper-left panel:* invariant mass distribution of the  $\ell^+\ell^-$  pair (step 2, HS scenario); *Upper-right panel:* di-jet invariant mass distribution from  $\tilde{\chi}_1^\pm$  (step 3, HS scenario); *Lower panel:* invariant mass distribution of the  $\ell^+\ell^-$  pair (step 3, HS scenario).

- (a)  $p_{T1,2} > 20, 10$  GeV on the 2 jets;
- (b)  $p_{T1,2} > 20, 10$  GeV on the 2 leptons;
- (c)  $\cancel{E}_T > 50$  GeV.

The di-jet invariant mass distribution is reported in fig. 11 (upper-right panel). As can be seen by the length of its tail, the background contribution is quite severe for this channel even after the above cuts. The fitted endpoint allows to estimate  $m_{\tilde{\chi}_1^\pm} - m_{\tilde{\chi}_1^0}$  to be 78(11) GeV, whose central value is 35 % larger than the true value 58 GeV. So, because of this systematics, the accuracy in the determination of  $m_{\tilde{\chi}_1^\pm}$  turns out to be not as good as for the other mass determinations in the HS scenario.

In addition, we can check  $m_{\tilde{\chi}_2^0} - m_{\tilde{\chi}_1^0}$  as obtained in step 2 by constructing the invariant mass of the two leptons. Fig. 11 (lower panel) displays the corresponding distribution, showing again the quite clear endpoint at 60 GeV, though it is more smeared by backgrounds than the distribution in step 2.

## 5. Conclusions and Outlook

We have explored, in the concrete example of Yukawa-unified SUSY GUTs, to which extent a quantitative determination of the lightest part of the SUSY spectrum is practicable with LHC data. Specifically, we have considered two representative scenarios, both viable in the light of all existing data, but characterized by some notable differences in the SUSY spectra (summarized in table 1), that arguably can be told apart only via their direct measurement.

We have elaborated a mass-determination strategy based on the observation of kinks in the kinematic variable  $m_{T2}$ , namely the so-called  $m_{T2}$ -kink method. This method is especially suitable for our purposes, as it does not rely on the presence of long decay chains, which are not achievable at the LHC within our considered classes of models.

	Quantity	Result (GeV)
LS scenario	$m_{\tilde{g}}$	$395 \pm 16$
	$m_{\tilde{\chi}_1^\pm}$	$109 \pm 17$
	$m_{\tilde{\chi}_1^0}$	$57 \pm 17$
	$m_{\tilde{\chi}_2^0}$	$107 \pm 18$
	$m_{\tilde{t}_1}$	$206 \pm 17$
HS scenario	$m_{\tilde{g}}$	$456 \pm 15$
	$m_{\tilde{\chi}_1^\pm}$	$144 \pm 20$
	$m_{\tilde{\chi}_1^0}$	$66 \pm 16$
	$m_{\tilde{\chi}_2^0}$	$126 \pm 16$

**Table 5:** Mass determinations within our strategy, to be compared with table 1.

a statistical error always around 20 GeV and a systematics somewhat larger for the HS scenario.

Our worked example of Yukawa-unified SUSY GUTs may offer a useful playground for dealing with other theories which predict similar patterns of SUSY spectra.

Of course, a number of issues are left open by the present study. First, although we have been focusing on mass determinations, it is also of crucial importance to determine the spin of any SUSY particle produced at the LHC. To this aim, we just note here that the approach of ref. [71], whereby the invisible particle momenta are reconstructed with  $m_{T2}$  in order to determine the mother-particle spin, may be applied to the decay of pair-produced gluinos in the scenarios of [10, 16], from which the gluino spin might be read off.

Further issues are more specifically concerned with mass measurements and the precision achieved in their determination. For example, a first relevant question is that of the luminosity needed for the discovery of either channel. A rough extrapolation of our results indicates that about 5 to 10  $\text{fb}^{-1}$  of data would be sufficient to obtain a statistical error on the mass determinations of about 50 GeV. This amount of data would therefore suffice

We have studied in detail our strategy on 100  $\text{fb}^{-1}$  of data collected at 14 TeV  $p$ -on- $p$  collisions, using Pythia 6. We have also simulated detector-level effects via PGS4, with the aim of conveying a hopefully realistic idea of how large a degradation is expected in real signals.

We were able to determine the masses of the gluino, of the lightest chargino, of the first two neutralinos for both scenarios considered, and also the mass of the lightest stop for the scenario where this mass is below the gluino's. Our results are summarized in table 5, as obtained through a global fit to the outcomes (masses or functions thereof) of the various steps described in section 4 for either scenario. The results in table 5 display a good agreement with the corresponding true values in table 1,

for a  $5\sigma$  discovery of at least the heavier among the particles listed in Table 5 for either scenario.

We note as well that we did not try and exploit here the approach of ref. [72], that has been proposed as a strategy to make the endpoint structure more prominent, and that might be able to reduce the systematic errors in the identification of the endpoint position of the kinematic variables considered in our analysis. Pursuing these, more refined strategies could also offer a handle to address the case of lower needed luminosities, where the signal reach may be increased by also using more optimized cuts, or allow to implement our strategy to data from Tevatron Run II and from the LHC running at center-of-mass energies below the design one.

## Acknowledgments

KC and DG warmly acknowledge the CERN Theory Institute and the Galileo Galilei Institute (Florence, Italy), where initial discussions have taken place. DG is especially indebted to R. Franceschini, M.-H. Genest, S. Kraml, F. Mescia, M. Pierini, S. Sekmen and D.M. Straub for valuable feedback. KC, SHI and CBP are supported by the KRF grants funded by the Korean Government (KRF-2007-341-C00010 and KRF-2008-314-C00064) and KOSEF grant funded by the Korean Government (No. 2009-0080844). The work of DG is supported by the DFG Cluster of Excellence ‘Origin and Structure of the Universe’.

## References

- [1] T. Blazek, R. Dermisek, and S. Raby, *Predictions for Higgs and SUSY spectra from  $SO(10)$  Yukawa unification with  $\mu > 0$* , *Phys. Rev. Lett.* **88** (2002) 111804, [[hep-ph/0107097](#)].
- [2] T. Blazek, R. Dermisek, and S. Raby, *Yukawa unification in  $SO(10)$* , *Phys. Rev.* **D65** (2002) 115004, [[hep-ph/0201081](#)].
- [3] H. Baer and J. Ferrandis, *Supersymmetric  $SO(10)$  GUT models with Yukawa unification and a positive mu term*, *Phys. Rev. Lett.* **87** (2001) 211803, [[hep-ph/0106352](#)].
- [4] K. Tobe and J. D. Wells, *Revisiting top-bottom-tau Yukawa unification in supersymmetric grand unified theories*, *Nucl. Phys.* **B663** (2003) 123–140, [[hep-ph/0301015](#)].
- [5] D. Auto *et. al.*, *Yukawa coupling unification in supersymmetric models*, *JHEP* **06** (2003) 023, [[hep-ph/0302155](#)].
- [6] C. Balazs and R. Dermisek, *Yukawa coupling unification and non-universal gaugino mediation of supersymmetry breaking*, *JHEP* **06** (2003) 024, [[hep-ph/0303161](#)].
- [7] D. Auto, H. Baer, A. Belyaev, and T. Krupovnickas, *Reconciling neutralino relic density with Yukawa unified supersymmetric models*, *JHEP* **10** (2004) 066, [[hep-ph/0407165](#)].
- [8] M. Albrecht, W. Altmannshofer, A. J. Buras, D. Guadagnoli, and D. M. Straub, *Challenging  $SO(10)$  SUSY GUTs with family symmetries through FCNC processes*, *JHEP* **10** (2007) 055, [[arXiv:0707.3954](#)].
- [9] H. Baer, S. Kraml, S. Sekmen, and H. Summy, *Dark matter allowed scenarios for Yukawa-unified  $SO(10)$  SUSY GUTs*, *JHEP* **03** (2008) 056, [[arXiv:0801.1831](#)].

- [10] W. Altmannshofer, D. Guadagnoli, S. Raby, and D. M. Straub, *SUSY GUTs with Yukawa unification: a go/no-go study using FCNC processes*, *Phys. Lett.* **B668** (2008) 385–391, [[arXiv:0801.4363](#)].
- [11] H. Baer, S. Kraml, S. Sekmen, and H. Summy, *Prospects for Yukawa Unified SO(10) SUSY GUTs at the CERN LHC*, *JHEP* **10** (2008) 079, [[arXiv:0809.0710](#)].
- [12] H. Baer, M. Haider, S. Kraml, S. Sekmen, and H. Summy, *Cosmological consequences of Yukawa-unified SUSY with mixed axion/axino cold and warm dark matter*, *JCAP* **0902** (2009) 002, [[arXiv:0812.2693](#)].
- [13] S. Antusch and M. Spinrath, *Quark and lepton masses at the GUT scale including SUSY threshold corrections*, *Phys. Rev.* **D78** (2008) 075020, [[arXiv:0804.0717](#)].
- [14] S. Antusch and M. Spinrath, *New GUT predictions for quark and lepton mass ratios confronted with phenomenology*, [arXiv:0902.4644](#).
- [15] I. Gogoladze, R. Khalid, and Q. Shafi, *Yukawa Unification and Neutralino Dark Matter in  $SU(4)_c \times SU(2)_L \times SU(2)_R$* , *Phys. Rev.* **D79** (2009) 115004, [[arXiv:0903.5204](#)].
- [16] D. Guadagnoli, S. Raby, and D. M. Straub, *Viable and testable SUSY GUTs with Yukawa unification: the case of split trilinears*, [arXiv:0907.4709](#).
- [17] H. Baer, S. Kraml, and S. Sekmen, *Is 'just-so' Higgs splitting needed for  $t - b - \tau$  Yukawa unified SUSY GUTs?*, *JHEP* **09** (2009) 005, [[arXiv:0908.0134](#)].
- [18] H. Baer, S. Kraml, A. Lessa, S. Sekmen, and H. Summy, *Beyond the Higgs boson at the Tevatron: Detecting gluinos from Yukawa-unified SUSY*, *Phys. Lett.* **B685** (2010) 72–78, [[arXiv:0910.2988](#)].
- [19] H. Baer, S. Kraml, A. Lessa, and S. Sekmen, *Testing Yukawa-unified SUSY during year 1 of LHC: the role of multiple b-jets, dileptons and missing  $E_T$* , *JHEP* **02** (2010) 055, [[arXiv:0911.4739](#)].
- [20] T. Banks, *Supersymmetry and the Quark Mass Matrix*, *Nucl. Phys.* **B303** (1988) 172.
- [21] M. Olechowski and S. Pokorski, *Hierarchy of Quark Masses in the Isotopic Doublets in  $N=1$  Supergravity Models*, *Phys. Lett.* **B214** (1988) 393.
- [22] S. Pokorski, *On weak isospin breaking in the quark mass spectrum*, *Nucl. Phys. Proc. Suppl.* **13** (1990) 606–608.
- [23] B. Ananthanarayan, G. Lazarides, and Q. Shafi, *Top mass prediction from supersymmetric GUTs*, *Phys. Rev.* **D44** (1991) 1613–1615.
- [24] Q. Shafi and B. Ananthanarayan, *Will LEP-2 narrowly miss the Weinberg-Salam Higgs boson?*, . Presented at Trieste Summer School, Trieste, Italy, Jun 15 - Aug 14, 1991.
- [25] S. Dimopoulos, L. J. Hall, and S. Raby, *A Predictive framework for fermion masses in supersymmetric theories*, *Phys. Rev. Lett.* **68** (1992) 1984–1987.
- [26] S. Dimopoulos, L. J. Hall, and S. Raby, *A Predictive ansatz for fermion mass matrices in supersymmetric grand unified theories*, *Phys. Rev.* **D45** (1992) 4192–4200.
- [27] G. W. Anderson, S. Raby, S. Dimopoulos, and L. J. Hall, *Precise predictions for  $m_t$ ,  $V_{cb}$ , and  $\tan \beta$* , *Phys. Rev.* **D47** (1993) 3702–3706, [[hep-ph/9209250](#)].
- [28] B. Ananthanarayan, G. Lazarides, and Q. Shafi, *Radiative electroweak breaking and sparticle spectroscopy with  $\tan \beta$  approximately =  $m(t) / m(b)$* , *Phys. Lett.* **B300** (1993) 245–250.



- [29] G. Anderson, S. Raby, S. Dimopoulos, L. J. Hall, and G. D. Starkman, *A Systematic  $SO(10)$  operator analysis for fermion masses*, *Phys. Rev.* **D49** (1994) 3660–3690, [[hep-ph/9308333](#)].
- [30] B. Ananthanarayan, Q. Shafi, and X. M. Wang, *Improved predictions for top quark, lightest supersymmetric particle, and Higgs scalar masses*, *Phys. Rev.* **D50** (1994) 5980–5984, [[hep-ph/9311225](#)].
- [31] L. J. Hall, R. Rattazzi, and U. Sarid, *The top quark mass in supersymmetric  $SO(10)$  unification*, *Phys. Rev.* **D50** (1994) 7048–7065, [[hep-ph/9306309](#)].
- [32] G. D’Ambrosio, G. F. Giudice, G. Isidori, and A. Strumia, *Minimal flavour violation: An effective field theory approach*, *Nucl. Phys.* **B645** (2002) 155–187, [[hep-ph/0207036](#)].
- [33] G. Anderson *et. al.*, *Motivations for and implications of non-universal GUT- scale boundary conditions for soft SUSY-breaking parameters*, [hep-ph/9609457](#).
- [34] A. J. Barr and C. G. Lester, *A Review of the Mass Measurement Techniques proposed for the Large Hadron Collider*, [arXiv:1004.2732](#).
- [35] I. Hinchliffe, F. E. Paige, M. D. Shapiro, J. Soderqvist, and W. Yao, *Precision SUSY measurements at CERN LHC*, *Phys. Rev.* **D55** (1997) 5520–5540, [[hep-ph/9610544](#)].
- [36] H. Bachacou, I. Hinchliffe, and F. E. Paige, *Measurements of masses in SUGRA models at CERN LHC*, *Phys. Rev.* **D62** (2000) 015009, [[hep-ph/9907518](#)].
- [37] I. Hinchliffe and F. E. Paige, *Measurements in SUGRA models with large  $\tan(\beta)$  at LHC*, *Phys. Rev.* **D61** (2000) 095011, [[hep-ph/9907519](#)].
- [38] B. C. Allanach, C. G. Lester, M. A. Parker, and B. R. Webber, *Measuring sparticle masses in non-universal string inspired models at the LHC*, *JHEP* **09** (2000) 004, [[hep-ph/0007009](#)].
- [39] B. K. Gjelsten, D. J. Miller, 2, and P. Osland, *Measurement of SUSY masses via cascade decays for SPS 1a*, *JHEP* **12** (2004) 003, [[hep-ph/0410303](#)].
- [40] **LHC/LC Study Group** Collaboration, G. Weiglein *et. al.*, *Physics interplay of the LHC and the ILC*, *Phys. Rept.* **426** (2006) 47–358, [[hep-ph/0410364](#)].
- [41] B. K. Gjelsten, D. J. Miller, 2, and P. Osland, *Measurement of the gluino mass via cascade decays for SPS 1a*, *JHEP* **06** (2005) 015, [[hep-ph/0501033](#)].
- [42] C. G. Lester, M. A. Parker, and M. J. White, 2, *Three body kinematic endpoints in SUSY models with non- universal Higgs masses*, *JHEP* **10** (2007) 051, [[hep-ph/0609298](#)].
- [43] B. K. Gjelsten, D. J. Miller, 2, P. Osland, and A. R. Raklev, *Mass Determination in Cascade Decays Using Shape Formulas*, *AIP Conf. Proc.* **903** (2007) 257–260, [[hep-ph/0611259](#)].
- [44] **The ATLAS** Collaboration, G. Aad *et. al.*, *Expected Performance of the ATLAS Experiment - Detector, Trigger and Physics*, [arXiv:0901.0512](#).
- [45] M. Burns, K. Kong, K. T. Matchev, and M. Park, *Using Subsystem  $MT_2$  for Complete Mass Determinations in Decay Chains with Missing Energy at Hadron Colliders*, *JHEP* **03** (2009) 143, [[arXiv:0810.5576](#)].
- [46] M. M. Nojiri, G. Polesello, and D. R. Tovey, *Proposal for a new reconstruction technique for SUSY processes at the LHC*, [hep-ph/0312317](#).
- [47] K. Kawagoe, M. M. Nojiri, and G. Polesello, *A new SUSY mass reconstruction method at the CERN LHC*, *Phys. Rev.* **D71** (2005) 035008, [[hep-ph/0410160](#)].

- [48] H.-C. Cheng, J. F. Gunion, Z. Han, G. Marandella, and B. McElrath, *Mass Determination in SUSY-like Events with Missing Energy*, *JHEP* **12** (2007) 076, [[arXiv:0707.0030](#)].
- [49] M. M. Nojiri, G. Polesello, and D. R. Tovey, *A hybrid method for determining SUSY particle masses at the LHC with fully identified cascade decays*, *JHEP* **05** (2008) 014, [[arXiv:0712.2718](#)].
- [50] H.-C. Cheng, D. Engelhardt, J. F. Gunion, Z. Han, and B. McElrath, *Accurate Mass Determinations in Decay Chains with Missing Energy*, *Phys. Rev. Lett.* **100** (2008) 252001, [[arXiv:0802.4290](#)].
- [51] W. S. Cho, K. Choi, Y. G. Kim, and C. B. Park, *Gluino Stransverse Mass*, *Phys. Rev. Lett.* **100** (2008) 171801, [[arXiv:0709.0288](#)].
- [52] B. Gripaios, *Transverse Observables and Mass Determination at Hadron Colliders*, *JHEP* **02** (2008) 053, [[arXiv:0709.2740](#)].
- [53] A. J. Barr, B. Gripaios, and C. G. Lester, *Weighing Wimps with Kinks at Colliders: Invisible Particle Mass Measurements from Endpoints*, *JHEP* **02** (2008) 014, [[arXiv:0711.4008](#)].
- [54] W. S. Cho, K. Choi, Y. G. Kim, and C. B. Park, *Measuring superparticle masses at hadron collider using the transverse mass kink*, *JHEP* **02** (2008) 035, [[arXiv:0711.4526](#)].
- [55] M. M. Nojiri, Y. Shimizu, S. Okada, and K. Kawagoe, *Inclusive transverse mass analysis for squark and gluino mass determination*, *JHEP* **06** (2008) 035, [[arXiv:0802.2412](#)].
- [56] W. S. Cho, K. Choi, Y. G. Kim, and C. B. Park, *Mass and Spin Measurement with  $M_{T2}$  and MAOS Momentum*, [arXiv:0909.4853](#).
- [57] H.-C. Cheng and Z. Han, *Minimal Kinematic Constraints and  $MT_2$* , *JHEP* **12** (2008) 063, [[arXiv:0810.5178](#)].
- [58] P. Konar, K. Kong, K. T. Matchev, and M. Park, *Superpartner Mass Measurement Technique using 1D Orthogonal Decompositions of the Cambridge Transverse Mass Variable  $M_{T2}$* , *Phys. Rev. Lett.* **105** (2010) 051802, [[arXiv:0910.3679](#)].
- [59] C. G. Lester and D. J. Summers, *Measuring masses of semiinvisibly decaying particles pair produced at hadron colliders*, *Phys. Lett.* **B463** (1999) 99–103, [[hep-ph/9906349](#)].
- [60] A. Barr, C. Lester, and P. Stephens,  *$m(T_2)$  : The Truth behind the glamour*, *J. Phys.* **G29** (2003) 2343–2363, [[hep-ph/0304226](#)].
- [61] M. M. Nojiri, K. Sakurai, Y. Shimizu, and M. Takeuchi, *Handling jets + missing ET channel using inclusive  $mT_2$* , *JHEP* **10** (2008) 100, [[arXiv:0808.1094](#)].
- [62] A. J. Barr, B. Gripaios, and C. G. Lester, *Transverse masses and kinematic constraints: from the boundary to the crease*, *JHEP* **11** (2009) 096, [[arXiv:0908.3779](#)].
- [63] P. Konar, K. Kong, K. T. Matchev, and M. Park, *Dark Matter Particle Spectroscopy at the LHC: Generalizing  $MT_2$  to Asymmetric Event Topologies*, *JHEP* **04** (2010) 086, [[arXiv:0911.4126](#)].
- [64] T. Han, I.-W. Kim, and J. Song, *Kinematic Cusps: Determining the Missing Particle Mass at the LHC*, [arXiv:0906.5009](#).
- [65] I.-W. Kim, *Algebraic Singularity Method for Mass Measurement with Missing Energy*, *Phys. Rev. Lett.* **104** (2010) 081601, [[arXiv:0910.1149](#)].

- [66] T. Sjostrand, S. Mrenna, and P. Z. Skands, *PYTHIA 6.4 Physics and Manual*, *JHEP* **05** (2006) 026, [[hep-ph/0603175](#)].
- [67] A. Djouadi, M. M. Muhlleitner, and M. Spira, *Decays of Supersymmetric Particles: the program SUSY-HIT (SUspect-SdecaY-Hdecay-InTerface)*, *Acta Phys. Polon.* **B38** (2007) 635–644, [[hep-ph/0609292](#)].
- [68] **CMS** Collaboration, G. L. Bayatian *et. al.*, *CMS technical design report, volume II: Physics performance*, *J. Phys.* **G34** (2007) 995–1579.
- [69] J. Conway *et al.*, *PGS4, Pretty Good Simulation of high energy collisions*.
- [70] C. Lester and A. Barr, *MTGEN : Mass scale measurements in pair-production at colliders*, *JHEP* **12** (2007) 102, [[arXiv:0708.1028](#)].
- [71] W. S. Cho, K. Choi, Y. G. Kim, and C. B. Park,  *$M_{T2}$ -assisted on-shell reconstruction of missing momenta and its application to spin measurement at the LHC*, *Phys. Rev.* **D79** (2009) 031701, [[arXiv:0810.4853](#)].
- [72] W. S. Cho, J. E. Kim, and J.-H. Kim, *Amplification of endpoint structure for new particle mass measurement at the LHC*, [arXiv:0912.2354](#).